Dipl. Ing. Ernst Wiemann,
Bad Hersfeld

Component-Based Determination of Noise Levels

Calculation and upscaling of fan noise levels from model measurements using similarity laws

Fan operating noise can be divided into three basic source mechanisms for the sake of analytical transparency. By converting the source characteristics for a given fan on the basis of physical laws, it is possible to calculate the acoustic emissions of every identical model by a mere combination of these components. The calculation model employed yields a frequency analysis at the same time. Considering each source individually will facilitate the identification of superimposition effects and other phenomena.

The influencing factors computed for each source provide very useful standards of comparison when related to a flow velocity in a uniform reference cross-section.

The research efforts described herein were prompted by customer demand for ever more exacting data on anticipated noise levels of proposed fans. This problem had to be resolved for a broad portfolio of centrifugal fans with impeller ratios of 0.7 < d1/D2 < 0.2, blade outlet angles of 20 < ß2 < 90 deg., and blade numbers from 6 < Z < 17. In addition, an entire range of axial-flow fans had to be considered.

The model measurements were initially conducted by the enveloping surface method in front of the intake opening. Upon emergence of the in-duct method in 1977 [1], the latter was employed. During some of the measurements, fan speeds (rpm) were varied through the largest possible range.

Across the broad line-up of fans examined, the conversion methods known at the time yielded acceptable results only for the linear cumulative sound level. The measurements conducted at various speeds confirmed the different behaviour of individual tones and flow noise that was alredy known to exist at that time.

In recent years the subject has been addressed by a number of researchers. However, it is with good reason that Bommes writes: “According to Lighthill and other authors, the aerodynamic formation of tonal components which are a determinant of fan noise can be described in qualitative terms, but quantitative statements cannot be derived from this theory which is based on three typical elementary sources (monopole, dipole, quadrupole). This is due to the highly complex flow processes taking place inside the fan”.

References [4 and 12] are concerned with quantitative findings for one component of the overall sound spectrum, i.e., blade sound. These findings are calculated from flow field variables.

Bommes, in reference [3] and subsequent publications, examines the total acoustic power output. However, given the highly different behaviour of the individual sound sources, he is forced to work with different Mach number exponents calculated individually from measurements.

In reference [11], measurements on fans of the same model are examined separately for rotational sound and noise. These studies show a high degree of similarity between system frequency responses. While the levels for individual tones vary greatly as a function of the Helmholtz number, the differences in noise are minimal. Formulas for conversion to other speeds and nominal sizes are given both for individual frequency (Strouhal number) components as a function of the Helmholtz number and for the total acoustic power output. In the latter case, a Mach number exponent is used once again but is fixed this time since the investigation is carried out on fans of one specific model.

In the present work, the division of the rotor noise frequency spectrum suggested in [2] (Fig. 1) has prompted the author to split the measured third-octave levels into the components shown and to establish a separate law for each component. Accordingly, a program was developed to normalize the measured values before comparing them to the relevant basic curves.

Single tone

The single tone 1 (rotational sound) with its multiple 2 constitutes a forced

Symbols

D_2	Impeller outside diameter
d_1	Blade inlet diameter
β_2	Blade outlet angle
Z	Number of blades
U_2	Outer peripheral speed
U_0	Reference outer peripheral speed (1 m/s)
σ	Tip speed ratio
φ	Volume number $V/U_2 \cdot D_2^2 \cdot \pi/4$
β_{Bez}	Volume number $V/U_2 \cdot S_{Bez}$
φ_0	Reference volume number (1 –)
v	Flow velocity S_{Bez}
S_{Bez}	Cross-section of flow in the impeller inlet area
S	Reference cross-sections (1 m²)
$L_{W\,rel}$	Acoustic power level for one third-octave band
$L_{W\,spez}$	Specific acoustic power level for one third-octave band
Bandwidth	Width of the respective third-octave band
ϱ	Density
ϱ_0	Reference density (1,2 kg/m³)
C	Sound velocity
C_0	Reference sound velocity (340 m/s)
f	Frequency
He_{NG}	Helmholtz number obtained for the nominal diameter

oscillation having a frequency that can be calculated from the product of the speed (rpm) times the number of blades. This is a monopole source produced by a mass flow varying over time [5]. According to [6] this parameter is dependent on the fourth power of the mean flow velocity. Since the flow velocity and peripheral speed change proportionally for a specific operating point, the peripheral speed u2 can be used in the calculation for simplicity's sake. The normalized level of the single tones can thus be calculated as

$$L_{W\,spez} = (L_{W\,rel} - 10\log(\varphi_{Bez} \cdot S_{Bez} \cdot u_2^4) - 10\log(\varrho/c))$$ less the noise portion[1])

As described extensively in [3], the dependence of single tone levels on this law is masked to a great extent by natural resonance. In Fig. 2, the normalized level of single tones obtained by narrow-band measurements is plotted over the Helmholtz number. For this purpose the levels of the 1st and 2nd upper harmonic were raised by 10 and 15 dB, respectively, to ensure comparability.

Flow noise

Flow noise (Fig. 3) is produced, according to [5], by the non-steady interaction of forces between the flow medium and the impeller blades or deflecting or decelerating elements such as guide vanes. It is a dipolar source, which is reportedly [6] a function of the sixth power of the peripheral speed. The sickle-shaped acoustic component representing flow noise in Fig. 1 is clearly identifiable in the frequency analysis of the axial-flow fan (Fig. 7). The use of this sickle-curve as a standardized reference curve (expressed by a squared hyperbola) therefore suggested itself. Measurements conducted under varied fan rpm showed that the right-hand arm of the sickle is exactly dependent on the 6th power of the peripheral speed. However, this observation alone did not yet yield the intended solution, specifically when the results were converted to different nominal fan sizes. To resolve the problem, it was necessary to split the 6th

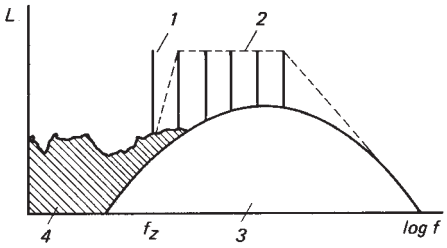

Fig. 1: Frequency range of rotor noise according to [**2**] (1 noise from rotational steady blade forces (sound of rotation), 2 noise from rotational non-steady periodic blade forces (interference sound), 3 noise from rotational non-steady random blade forces (turbulent outflow, turbulent boundary layer), 4 noise from rotational non-steady blade forces (turbulent inlet flow)

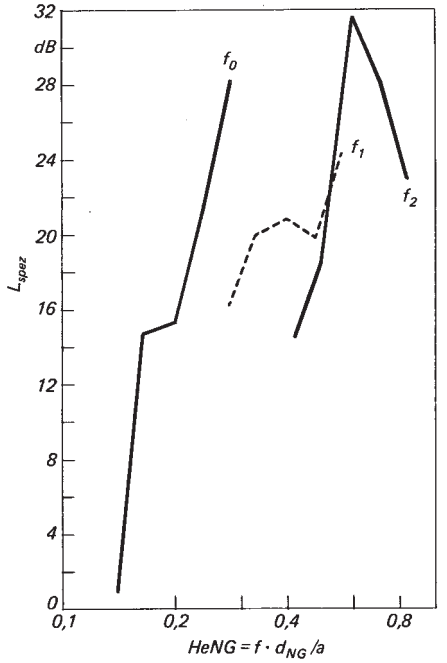

Fig. 2: Specific sound levels of the tonal portion K5 from narrow band measurements, plotted over the Helmholtz number

power into a dependence of the 4th power of the peripheral speed, and to shift the sickle as a function of the f/v ratio while additionally introducing the bandwidth into our calculation.

For the normalized one-third octave levels we can thus write

$$L_{W\,spez} = (L_{W\,rel} - 10\log(\varphi_{Bez} \cdot S_{Bez} \cdot u_2^4) - 10\log(\text{bandwidth}) - 10\log(\varrho^2/c^3)$$

The scale of the x-axis in Fig. 3 then becomes

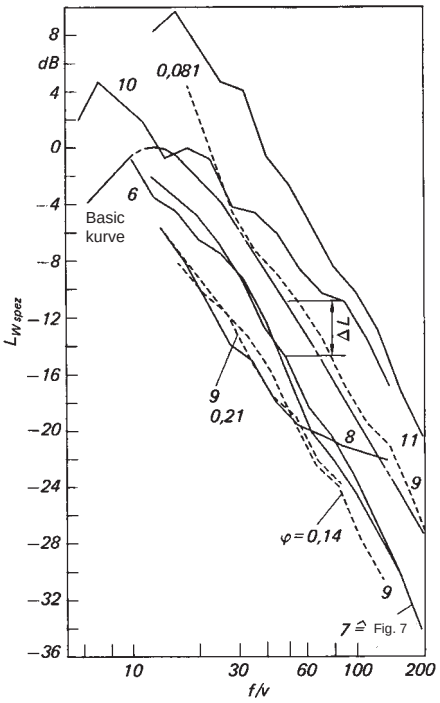

Fig. 3: Normalized one-third octave sound levels in the flow noise range, plotted over the ratio of frequency to reference flow velocity from the measurement documented in Fig. 6 to 11

$$\frac{f}{v} = \frac{f \cdot \varphi_0}{u_2 \cdot \varphi}$$

For v it was necessary to insert a flow velocity that would yield comparable velocities in the impeller throughout all model series. It was decided to use the velocity across the nominal cross-section, related to the impeller inlet, which has the additional advantage of being easily calculable from $v = u_2 \cdot \varphi_{Bez} = u_2 \cdot v/u_2$. The constant φ_0 = 0,25 emerged during evolution of the program over time.

Fig. 3 shows the normalized basic curve as compared to the normalized measured values for various fans and nominal sizes. In the case of the two centrifugal fans, different nominal sizes were compared at the same throttling point in each case. Measurements on the real-life fan were carried out at a point before the open inlet opening. Both comparisons show a good coincidence between the model and the real-life unit. Deviations in the high frequency range observed on real-life fans with d1/D2 = 0.56 from this series are attributable to an additional sound source. Throttling to

the desired operating point was achieved with wooden slats on the outlet side. While the above comparison covers the range of the fan's optimum point, two additional throttling points to the far left and right of the throttling point were likwise included from the measurements on the model centrifugal fan (Fig. 9). For a high volume number of φ = 0.21 the measurements at the operating point barely deviate from the optimum. This reflects the inclusion of the volume number in our normalization as well as the reduced pressure increase, which implies less flow deflection in the cascade. By contrast, at the lower volume number the normalized levels are markedly higher since the elevated pressure increase translates into higher cascade loads. The more pronounced level increase at f/v = 17.5 is still influenced by the low-frequency range. All other values lie essentially parallel to the basic curve.

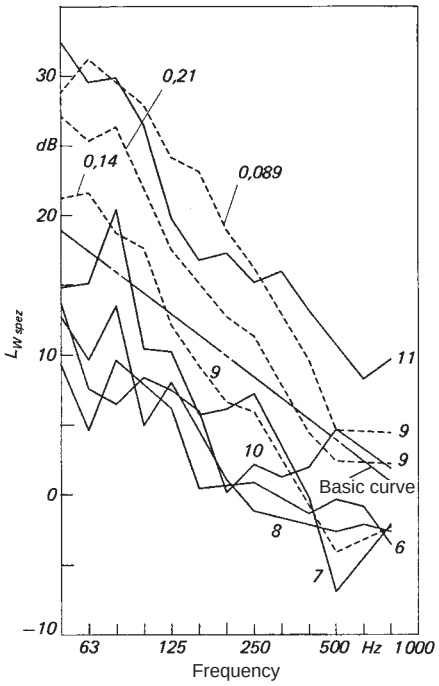

Fig. 4: Normalized one-third octave sound levels in the low-frequency range, plotted over frequency at the fan sound power levels documented in Figs. 6 to 11

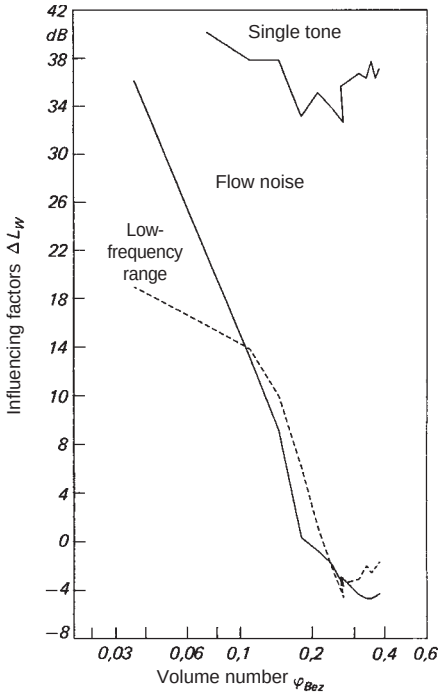

Fig. 5: Acoustic influencing factors L, calculated from readings on the centrifugal fan according to Fig. 7, plotted over the volume number

Same applies to the normalized values for the fan with forward curved blades which, as was to be anticipated, exhibited the highest levels since the highest cascade loads are also the highest in this case. The normalized readings for the axial-flow fan lay between those of the centrifugal fan and the fan with forward curved blades. This again is consistent with the cascade load situation. A curve drawn through the measuring points varies slightly from the basic curve in terms of position and shape; as a result, the basic curve must be adapted in the case of the axial-flow fan. Presumably this is due to the fact that the velocity conditions between the nominal cross-section and the cascade inlet differ from those of a centrifugal fan.

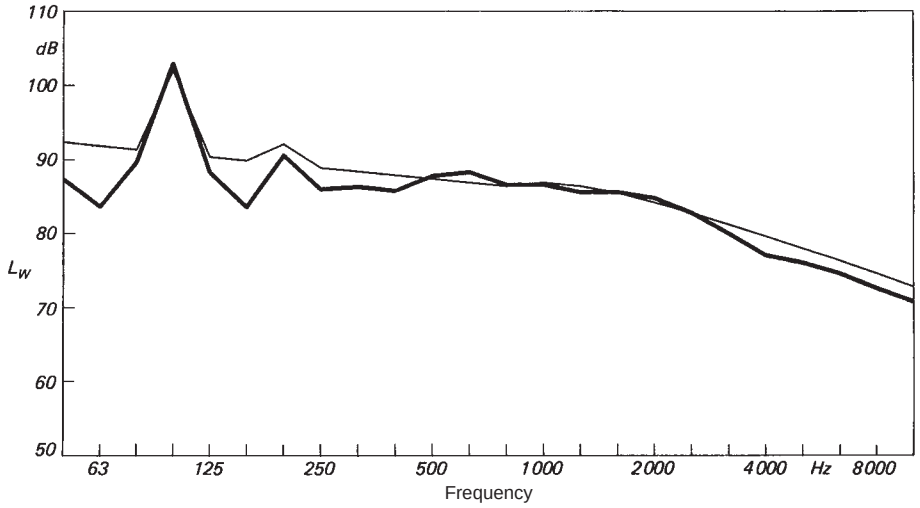

Fig. 6: Comparison between measured and calculated frequency range of the sound power output (centrifugal fan β_2 = 30°, D_2 = 1585 mm, d_1/D_2 = 0,7, φ = 0,22, σ = 0,58, z = 8)

Low-frequency range

Tones in the low-frequency range are attributed [5] to rotating non-steady blade forces resulting from inlet flow turbulence. Changing the distance of an upstream elbow to an axial-flow fan will alter this turbulence and hence, low-frequency noise output. Our own measurements on a centrifugal fan led to similar results. Sound levels in this range are essentially determined by turbulences generated in the impeller itself, e.g., as a result of inlet flow deflection. This is clearly evident from the progressive frequency analyses of the axial-flow fan (Fig. 10) without inlet deflectors (Fig. 10), centrifugal fans (Figs. 6 to 9), and fans with forward curved blades (Fig. 11) which exhibit the least favourable deflection situation and the highest noise level in this range. But it is also the accoustics it self that greatly influences the low-frequency range in particular is greatly influenced by the fundamentals of acoustics, as our measurements with a merely one-sided low-reflection termination demonstrated. These measurements revealed a dependence on the 4th power of the peripheral speed.

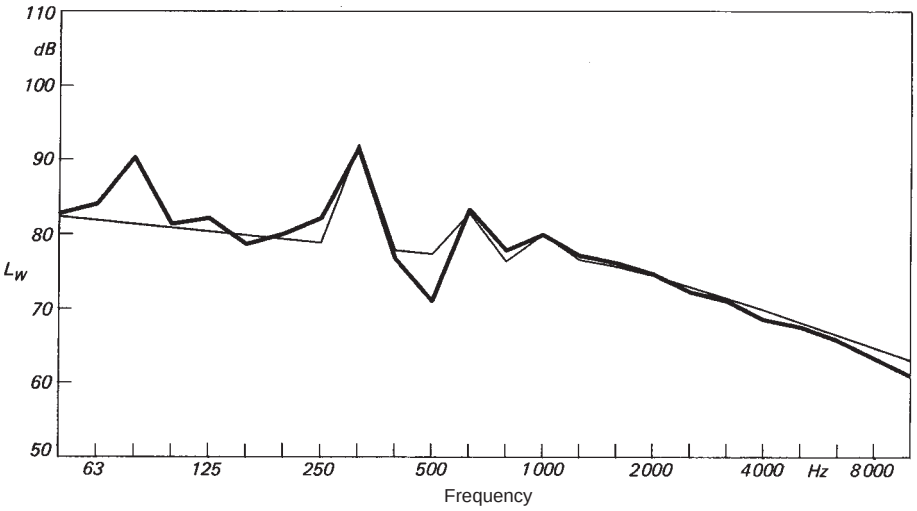

Fig. 7: Comparison between measured and calculated frequency range of the sound power output (centrifugal fan β_2 = 30°, Modell D_2 = 501 mm, d_1/D_2 = 0,7, φ = 0,22, σ = 0,58, z = 8)

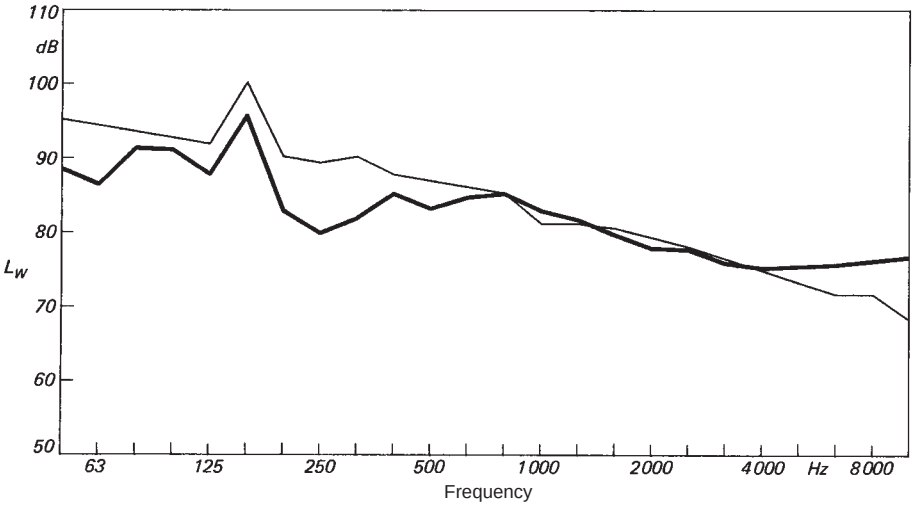

Fig. 8: Comparison between measured and calculated frequency range of the sound power output (centrifugal fan β_2 = 45°, D_2 = 1259 mm, d_1/D_2 = 0,56, φ = 0,14, σ = 0,37, z = 9)

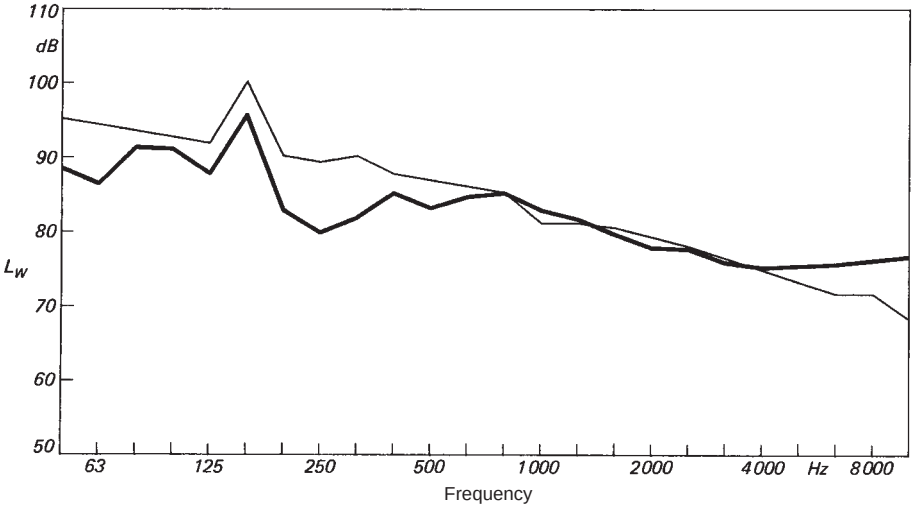

Fig. 9: Comparison between measured and calculated frequency range of the sound power output (centrifugal fan β_2 = 45°, model D_2 = 631 mm, d_1/D_2 = 0,56, φ = 0,14, σ = 0,37, z = 9)

The normalized one-third octave band noise level is calculated as

$$L_{W\,spez} = (L_{W\,rel} - 10\ log\ (\varphi_{Bez} \cdot S_{Bez} \cdot \upsilon_2^4)$$

$$- 10\ log\ (bandwidth)$$

$$- 10\ log\ (\varrho/c^3)$$

The frequency was not changed. Given the diversity of influences, a straight line was initially adopted as a basic curve to represent conditions in a generalized manner.

Fig. 4 plots the specific sound power levels emitted by the same fans in the low-frequency range, as was done for the flow noise in Fig. 3. As might be expected, the levels are lowest for the axial-flow fan since it operates without a flow deflection upstream of the cascade which might impact the cascade airflow itself.

The fan with forward curved blades shows the highest sound power levels. This, again, might have been anticipated since the flow will definitely stall at the point of deflection into the impeller. In the case of the centrifugal fan (Fig. 9), the readings for the three throttling points are again shown in the diagram. The minimum lies near the optimum value of the characteristic curve. From here the values rise to both sides, although the increase is more pronounced toward lower volume flows. This is due in part to the fact that the volume number φ appears the denominator in the equation for the normalized sound level; but also because shock pulse effects upon airflow entry into the cascade are more pronounced than with larger volume flows. A comparison of the two model measurements with the corresponding real-life fans shows a less satisfactory coincidence than was obtained for the flow noise. In the 63 Hz range, this effect is likely to reflect measuring errors committed on the real-life fan in terms of the probe distance and wavelength selected. The peak near 80 Hz on the 11.1/30 series model is attributable to a resonance depending on the length of the inlet nozzle. The cause of the deviations in the 250 Hz range has eluded clarification to date.

The program computes the mean sound level deviation ΔL, relying on the normalized readings and the basic curve in each case. In Fig. 5. these mean values are plotted over the outputs from Fig. 7. The minimum at $\varphi = 0.27$ will be noted; this value corresponds approximately to the fan's optimum point. At higher volume flows the influence rises only marginally. For higher volume flows, on the other hand, a pronounced increase can be observed; this reflects the fact that, firstly, absolute levels are higher in this range and, secondly, φ_{spec} appears in the denominator in the equation for $L_{Wspec.}$ The single tone, at $\varphi_{spec} = 0.036$, is masked by the flow noise.

To perform these calculations for a current fan of the same model, a second program proceeds "in reverse" using the same influencing factors and basic curves but reversing the normalizing process. As will be appreciated from Figs. 6 to 11, the curves appear somewhat "contrived"; nevertheless, they represent the measured values quite well, specifically in the flow noise (i.e., high-frequency) range. Single tones are likewise described quite consistently except where resonances are involved. A potential for improvement still exists, as has been demonstrated by individual calculations for centrifugal roof-units.

Summary

The development of this method, which, as initially noted, is based on analyses of numerous highly diverse measurements, has ultimately confirmed that the many-layered operating noise of fans can be reduced to a few basic physical patterns of the type described in [5] and [6]. An auxiliary variable such as the Mach number exponent is not needed for this purpose.

Absent from the abscissa of the f/v flow noise plot is the factor "d" of Strouhal's number, i.e., this is a dimensioned parameter. However, no further dependence has been identified. Presumably this is due to the manner of excitation by force transmission of the blades with their fairly large surface areas.

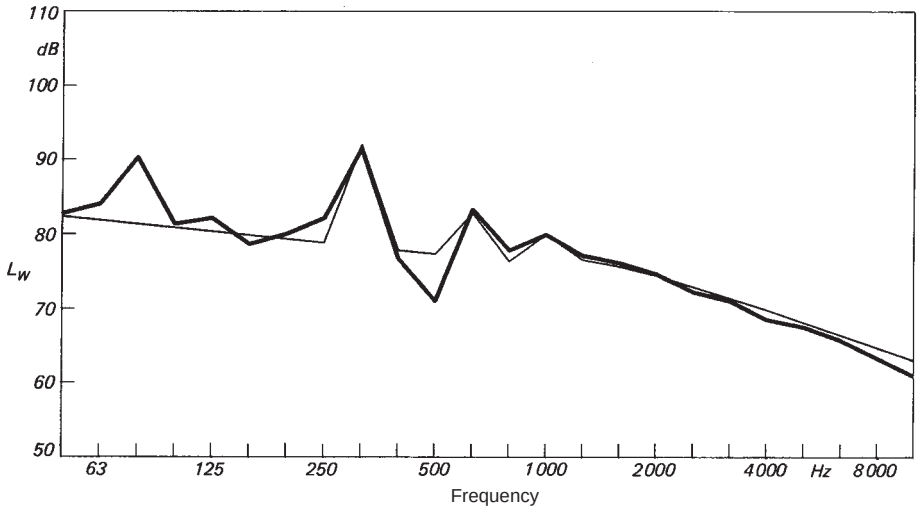

Fig. 10: Comparison between measured and calculated frequency range of the sound power output (axial-flow fan with outlet guide vanes, model D_2 = 400 mm, d_N/D_2 = 0,56, φ = 0,29, σ = 1,17, z = 12)

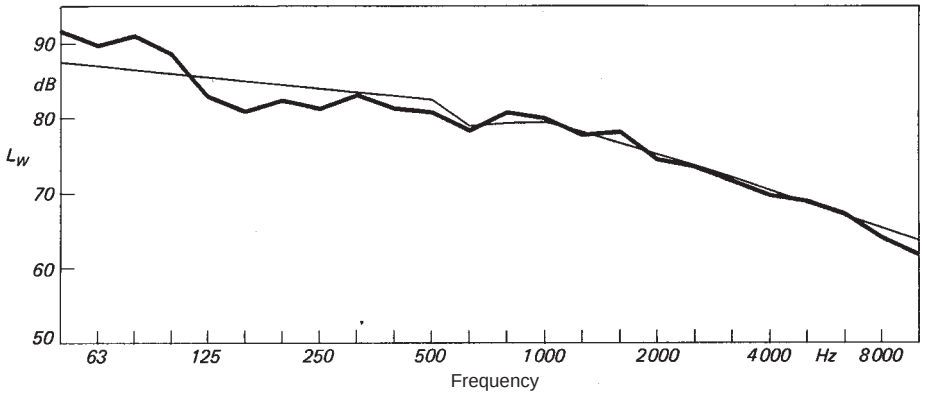

Fig. 11: Comparison between measured and calculated frequency range of the sound power output (fan with forward curved blades fan, model D_2 = 710 mm, φ = 0,48, σ = 0,33, z = 42)

In any case, the noise level increases along the characteristic line with the load per unit surface area. The levels exhibit no major variations, and the difference between measured and computed values is small. This is also true for the A-weighted total sound pressure level which is essentially determined by flow noise. Occasionally, secondary sources have been identified in the frequency range over 1000 Hz.

Single tone levels are determined by the mean velocity and velocity variations in the rotor wake downstream of the blades as it impinges on an obstruction such as the cut-off lip or outlet guide vanes. Here the sound level can be attenuated by enlarging the cut-off clearance according to [8] or by using more blades, as suggested by [3]. When increasing the number of blades, the trade-off between the resulting impact on the characteristic curve (instability according to [7] or increased susceptibility to "pumping") and the desired noise attenuation must be carefully weighed.

A single tone of the same level may stand out to varying extents against the surrounding background spectrum. In the extreme case of the fan with forward curved blades (Fig. 11), it will not be perceivable at all since it is drowned out by the vortex noise.

The sound level of individual tones can be reduced through fairly simple measures as detailed, e.g., in reference [10].

The vortex noise or low-frequency range is likely to be a result chiefly of

flow separation and cross-flow effects upstream of and in the impeller; at least, the response to all measures affecting such flow phenomena is most pronounced in this range. Influencing factors to be mentioned here by way of example include shock phenomena, flow separation occurring before or at the impeller inlet or at a specific variable inlet vane setting, and rotating stall.

These phenomena cannot be reproduced strictly true-to-scale by a model-based approach. As a result, deviations in the low-frequency range are significantly larger than with flow noise. In the range of very small Reynolds numbers, where cascade flow is greatly influenced according to [9], a dependence on the Reynolds tends to emerge. Concurrently, the characteristic curve values are reduced. Due to the A-weighting method, low-frequency attenuation steps will not usually be required except to meet more exacting specifications; however, if and when they do, cost and complexity of these measures will be vastly higher than for a single tone.

Critical review

The method described has given good results for years when utilized for its intended purpose, i.e., forecasting sound emission data in a project planning context. In the development of new fans, the verification capability gained with normalized frequency analyses of the type illustrated in Figs. 3 to 5 supplements the mere evaluation of characteristic curves, since flow irregularities in the range of the characteristic curve will be clearly revealed. The only identifiable drawback lies in the cost- and time-consuming measuring and evaluation process, especially if natural frequencies must be taken into account as well. However, given the universal comparability obtained, the method should also be well-suited for research purposes.

Literature

[1] DIN 45635, Part 9: Measurement of noise emitted by machines; airborne noise emission; in-duct method: method; basic method, draft standard, September 1977 / October 1985

[2] Wright, S.E.: Spectral trends in rotor noise generation, ALAA paper, No. 73-1033

[3] Bommes, L: Lärmminderung bei einem Radialventilator kleiner Schnelläufigkeit unter besonderer Berücksichtigung von Zungenform, Zungenabstand und Schaufelzahl [Noise attenuation on a centrifugal fan having a low tip speed ratio, with particular regard to cut-off lip shape, cut-off clearance and number of blades], HLH 31 (1980), No. 5 and 6

[4] Leist, H.: Untersuchung der Drehklangerzeugung von Radialventilatoren [Investigations into rotational sound formation in centrifugal fans], doctorate thesis by the author, Communications of the Institute of Flow Mechanics and Turbomachinery, University of Karlsruhe (TH), vol. 26/79

[5] Schmidt, L.: Der Einfluss eines 90°-Rohrkrümmers auf die Schallemission eines Axialventilators [Influence of a 90-deg. duct elbow on sound emissions of an axial-flow fan], Luft- und Kältetechnik 1976/6

[6] Cremer, Hubert: Vorlesungen über technische Akustik [Lectures in technical acoustics], 3rd ed., 1985

[7] Bodzian, Gotschalk: Kennlinienstabilität bei Radialventilatoren [Stability of characteristic curves in centrifugal Fans], FLT Report 3/1/23/75

[8] Leidel, W.: Einfluss von Zungenabstand und Zungenradius auf Kennlinie und Geräusch eines Radialventilators [Influence of the cut-off clearance and cut-off radius on the characteristic curves and noise emissions of a centrifugal fan], DLR-FB69-16 (1969)

[9] Eckert, B. and E. Schnell: Axial- und Radialkompressoren [Axial and radial flow compressors], Springer Publishing Co., 1961

[10] Neise, W. and G. H. Koopmann: Geräuschminderung bei Radialventilatoren durch λ/4-Resonatoren [Attenuation of centrifugal fan noise using λ/4 Resonators]. DFVLR-FB81-09 (1981), refer also to DAG 81 Conference Proceedings, p. 377/80

[11] Neise, W. and B. Basikow: Akustische Ähnlichkeitsgesetze bei Radialventilatoren [Acoustic similarity laws in centrifugal fans]

[12] Felsch, K. O. and Th. Sigel: Berechnung des Drehtons von Axialventilatoren aus den Stromfeldern [Calculating the rotational sound of axial-flow fans from flow fields], FLT Conference Paper, May 1985, Wiesbaden

[13] BABCOCK BSH Catalogues for Air Handling Fans and Components